Uniform Hierarchical Frameworks Patterned by Movable Magnetic Microparticles

Xiaolei Wang,[†] Hui Zhu,[†] Yi Bao,[†] Fan Yang,[†] and Xiurong Yang[†,*]

[†]State Key Laboratory of Electroanalytical Chemistry, Changchun Institute of Applied Chemistry, Chinese Academy of Sciences, 5625 Renmin Street, Changchun Jilin, 130022, China

ABSTRACT Inspired from the ancient movable type printing, we proposed a three-dimensional tunable method for the replicable patterning of uniform patterned framework. Different sized magnetic particles were utilized as the "type-heads" for patterning. The patterning area can be precisely defined by using commercial inkjet printer. Various materials, from multicomponent inorganic structures to well-defined microporous polymers, can be readily processed by this general strategy. As a practical example, we designed and constructed an intelligent multilevel hierarchy with versatile protective capabilities.

KEYWORDS: patterned structure · magnetic particles · microporous polymer · ZnO nanoarrays

Thirty years ago, when scientists took a deeper look at some natural surfaces (such as butterfly wings, lotus leaves, and gecko feet), they discovered intricate three-dimensional (3D) patterned structures. These exquisite structures endow their owners with fascinating properties.[1−8] For more than 15 years, researchers have tried to develop an appropriate fabrication technique for artificial patterned materials (APM).[9−13] Although numerous reports have appeared, many of them are still far from practical implementations. The widespread use of APM, though promising and fascinating, is still in its infancy.

The key to the popularization of APM is to develop a worthwhile approach to yield high quality and uniform products. Last year, we reported an interesting strategy of using biofilm as the nanostructure organizer.[14] This method was proved to be an efficient and low-cost approach for large-scale nanoengineering. However, those living microorganisms are too fragile and risky to be operated precisely. On the other hand, uniform products can only be obtained with difficulty by using this method. To guarantee the consistency of the patterning process, a more reliable alternative to the bacterium is desirable.

In theory, magnetic particles can be an attractive possibility for this purpose, as they can be synthesized in large quantities with precise diameters.[15−19] On the basis of this information, we designed a movable magnetic patterning (MMP) system with three-dimensional tunable capabilities. The original idea of MMP was derived from the ancient movable type printing technique. As depicted in Figure 1, magnetic microparticles were utilized here as the type-head for patterning. Filters with proper diameter holes were applied on the top of the target surface to maintain a uniform distribution of those magnetic microparticles. By reversing the magnetic orientation, the entire patterning and separation process could be accomplished in order. One fact worth mentioning is that magnetic microparticles are much more stable than microorganisms. Their movable abilities thus make them reusable, and thereby allow for a replicable patterning system. Consequently, complex and uniform APM could be duplicated in copies precisely.

RESULTS AND DISCUSSION

To illustrate the attractive idea of APM duplication, we selected solution-grown ZnO nanoarrays as the model system.[20,21] Several copies of them were patterned with the same batch of magnetic microparticles (Affimag PSC Magnetic Microspheres, 5 μm in diameter, purchased from BaseLine Company) in sequence. Among them, three samples were randomly selected to be studied by scanning electron microscopy (SEM). As depicted in Figure 2, well-ordered ZnO "nest" structures were patterned precisely on each substrate. No significant difference was observed between the samples. MMP technique thus exhibited remarkable accuracy and consistency, making it a

* Address correspondence to xryang@ciac.jl.cn.

Received for review January 30, 2011 and accepted March 2, 2011.

Published online March 02, 2011
10.1021/nn2003794

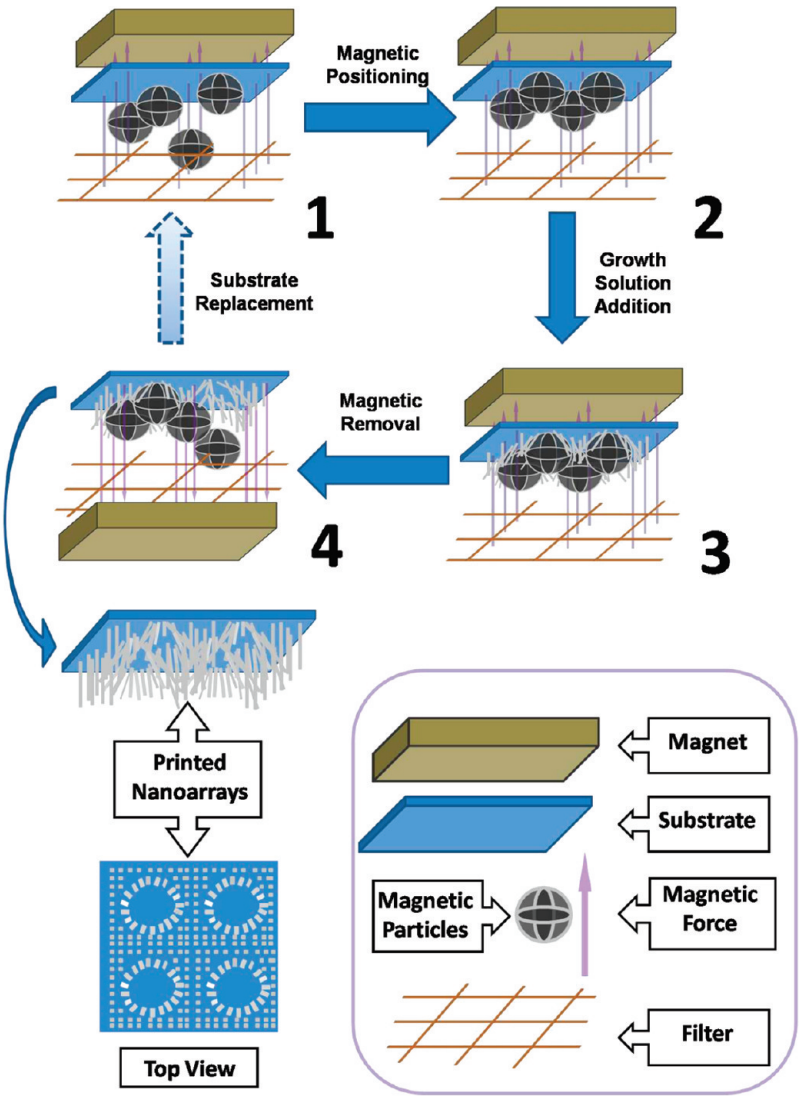

Figure 1. The schematic diagram of the MMP process. Magnetic microparticles, dispersed by the filter, were absorbed on the substrate by using magnet force. The growth manner of the subsequent nanostructure would then be converted by the spacial hindrances of the absorbed magnetic microparticles. As a result, by reversing the magnetic force direction, several magnetic microparticles shaped holes would be patterned on the nanostructure surface.

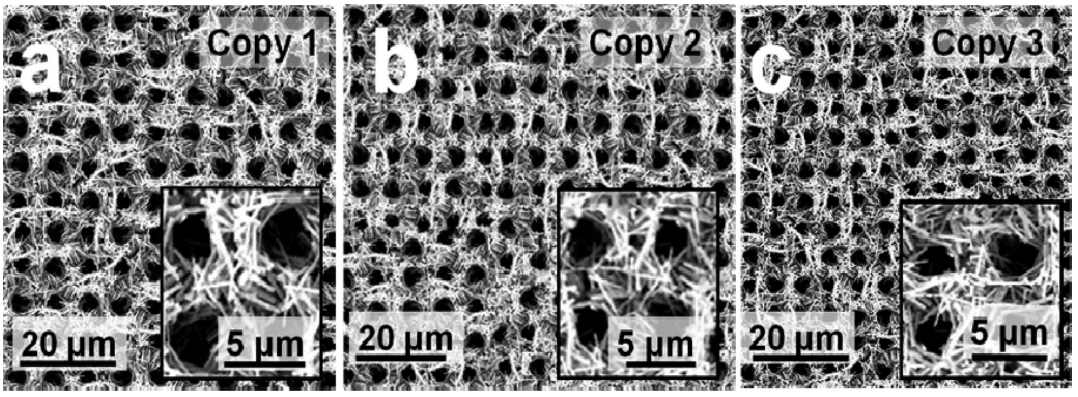

Figure 2. The SEM images of three copies of ZnO nest structures patterned with same batch of MMP. Inserts are enlarged views of the each image.

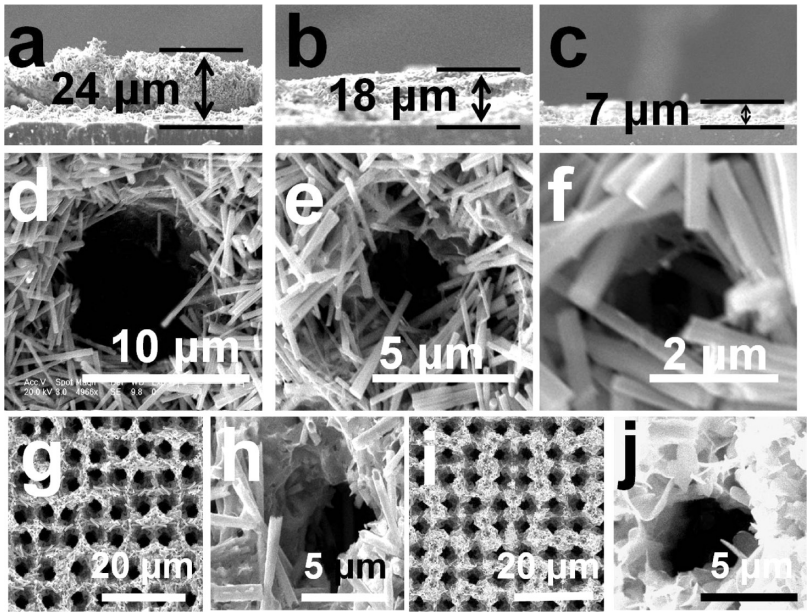

Figure 3. The three-dimensional adjustability and universality of MMP. (a−c) MMP manufactured APM with different thickness; (d−f) MMP manufactured APM with different nest diameters; (g) MMP manufactured APM of ZnO nanotubes, (h) the correponding-enlarged view of g; (i) MMP manufactured APM of In_2O_3 slices, (j) the corresponding-enlarged view of panel i.

suitable strategy for the volume production of complex devices. Moreover, the costs of laborious template making and post-treatment could be minimized. Compared with the conventional template masking technique, such characteristic would greatly improve the economic competitiveness of MMP.

Another fascinating feature of MMP is its three-dimensional adjustability. The desired pattern can be effectively modified in both vertical (thickness) and horizontal (in-plane diameter) directions. Still taking the above model, the thickness of the structure was decided by the reaction time (Figure 3a−c). Besides, the diameter of each ZnO nest (Figure 3d−f) could also be adjusted by varying the size of magnetic type-head (10, 5, and 2 μm). In an analogous manner, we patterned arrays of ZnO nanotubes (Figure 3g,h) and In_2O_3 slices (Figure 3i,j) on the surface of indium oxide−tin oxide (ITO) substrate. As expected, the MMP method exhibited a remarkable universality among samples and substrates. However, systematic SEM studies revealed that, a clear and uniform typing was difficult to realize once the diameter of type-head decreased below 1 μm. This threshold problem is probably inevitable when the size of type-head is close to the size of target material.

In addition to inorganic structures, MMP may also be used to process organic material. When an appropriate magnetic field was applied, magnetic microparticles would bump or even penetrate an organic membrane. In this case, by varying the magnetic microparticles size, microporous structures with defined pore diameters would be formed on the sample surface. A study was then carried out to validate this interesting assumption. One particularly challenging aspect of this work was to use a commercial inkjet printer to control the microporous distribution. Three different sized magnetic microparticles (Affimag PSC Magnetic Microspheres, 2, 5, and 10 μm) were placed in each cartridge as "inks" and patterned on the same surface of a PVC film (Figure 4). Patterns of 10 , 5, and 2 μm were printed by inks of 10, 5, and 2 μm sized magnetic microparticles, respectively. It was then studied by SEM and shown in Figure 5. As expected, three groups of well-defined microporous structures with different pore diameters were formed accurately at the desirable location. MMP thus can be applied to process different microporous organic membranes, which is a rising field in the forefront of membrane technology.

MMP even enables us to realize some optimized structures on different soft materials. For a practical example, we designed a new size recognition membrane and finally patterned it on the surface of a medical band-aid. This is also an extension of our previous work in which we organized a size recognition structure by using biofilm.[14] The as organized nest unit is larger than pathogenic bacteria but smaller than a human cell. It is thus possible to control the additive interaction on demand and provide both human cell protection and pathogenic bacteria killing properties. In this report, a magnetic particle was selected as a more reliable alternative to the fragile biofilm, and it was believed to form more uniform products with improved properties. As shown in Figure 6, MMP organized a multilevel hierarchy of ZnO nests (average diameter = 3.7 μm) loaded with several Ag decorated magnetic Fe_3O_4 "eggs" (average diameter =1.1 μm) (Supporting Information, Figure S3). Compared with

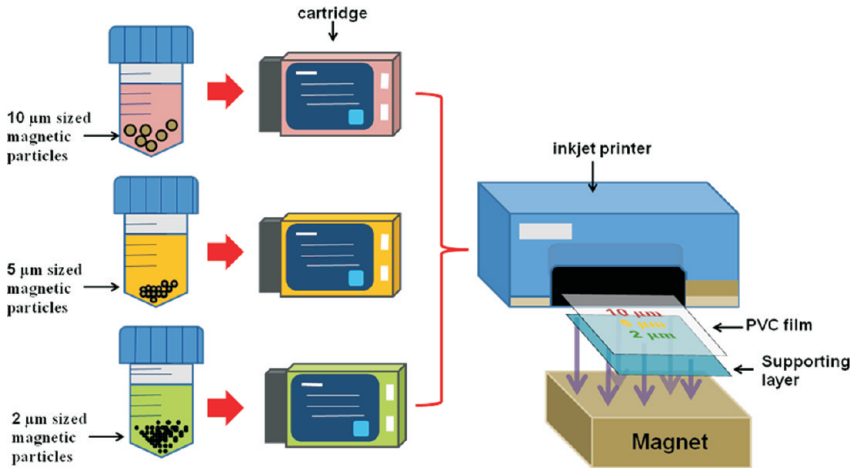

Figure 4. Schematic presentation of the MMP patterning process by using an inkjet printer. Three different sized magnetic microparticles (10, 5, and 2 μm) were used as inks and placed in three empty cartridges separately. Inkjet printer was employed to precisely control the patterning region. During patterning, a magnetic force was applied to drive the inks, so that they can bump or even penetrate the PVC film at the desired location. Various patterns formed by different pore sized microporous framework would then be generated on the PVC surface in a one-step process.

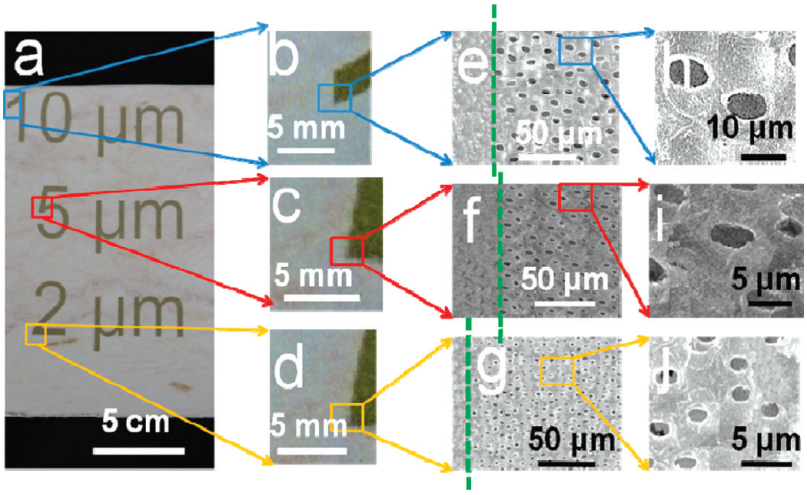

Figure 5. Microporous PVC film prepared by inkjet printer loaded with three different sized magnetic microparticles. Patterns of 10, 5, and 2 μm were patterned by inks of 10, 5, and 2 μm sized magnetic microparticles, respectively. (a) The optic image of the treated PVC film; (b−d) enlarged views of the selected region shown in panel a, respectively, (e,f) The SEM enlarged views of 10, 5, and 2 μm sized microporous framework from the selected surfaces. The green dot line represents the boundary between the patterned and the original area. (h−j) The detailed views of the selected area shown in panels e, f, and g, respectively.

the traditional size-recognition nests organized by biofilm (Supporting Information, Figure S4),[14] the upgrade versions were roughly 3 times larger, 2 times thicker, and 46 times denser. The summation of those improvements results in over 300-fold increases in effective area (Supporting Information, Table S1). Thereby, more invasive bacteria can be loaded and killed in such a modified structure. On the other hand, the thicker structure could decrease the undesirable side effect of Ag on larger sized human cells. To support our hypothesis, microbiological toxicity experiments on membranes made by MMP and biofilm were carried out by *Escherichia coli.* (*E.coli*), *S.aureus*, and HEK 293. The obtained data were summarized in Figure 7. As expected, these results demonstrated that MMP-modified membrane not only exerted a higher antibacterial activity against pathogenic bacteria but also exhibited a lower cytotoxicity to human cell.

The substitution of a Ag-decorated magnetic egg for pure Ag particles substantially lower the Ag dosage, minimizing both the toxicity and the cost of the membrane. More interestingly, we occasionally noticed that the new membrane could attenuate around 30% of the electromagnetic radiation (EMR) pulse from digital Global Systems for Mobile (GSM) telephones. And such an EMR shielding property can be substantially improved by adding the silver content to the substrate. (Supporting Information, Table S2). There has been growing public concern about the effects of EMR emitted by cellular phones on human health.[22]

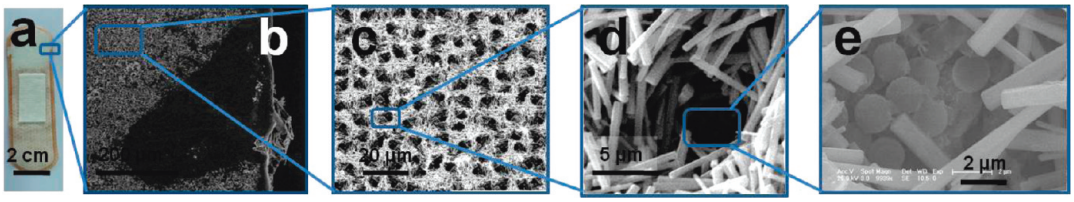

Figure 6. Optical and SEM images of a band-aid covered with a size-recognition membrane formed by ZnO nests loaded with Ag decorated magnetic eggs. (a) Optic image of the membrane covered band-aid, (b) SEM enlarged view of the band-aid substrate and the size-recognition membrane, (c) SEM enlarged view of the size-recognition membrane constructed by several nest units. (d) SEM enlarged view of a single nest unit formed by ZnO nanowires. (e) SEM detailed view of the Ag decorated magnetic eggs loaded at the bottom of the nest.

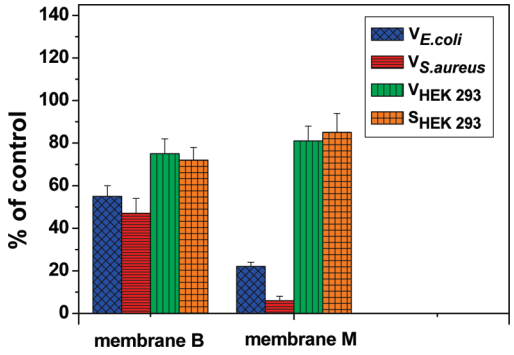

Figure 7. The microbiological toxicity comparison between the membrane made by biofilm (membrane B) and the membrane made by MMP (membrane M). $V_{E.coli}$, $V_{S.aureus}$ and V_{HEK293} represent the relative cell viability of *E.coli*, *S. aureus*, and HEK 293, respectively. S_{HEK293} represents the relative average succinic dehydrogenase (SDH) activity (mitochondrial function) of each HEK293 cell. For ease of comparison, each result on the control (conventional ZnO nanoarrays) was designated as 100% scale. The data are the mean of at least three independent experiments.

This low toxicity membrane can be used as a shielding material to minimize the possibly hazardous health risks associated with EMR. Since nanosized ZnO is also a low-toxic material with antiallergic[23,24] and ultraviolet (UV) blocking properties,[25] it is thus possible to upgrade various daily necessities (such as medical bandage, indoor wallpaper, and outdoor coat) with this breathable membrane to provide protection against pathogenic infection, allergic sensitization, UV-induced damage, and electromagnetic irradiation. It would be particularly suited for people working in high-risk areas. A middle-sized lab coat will cost no more than 45 g of this layer (15 μm in thickness), which is both physically and economically feasible.

CONCLUSION

In ancient time, the invention of movable type printing technique not only made reading cheaper, but also popularized education. Inspired from this great wisdom, we developed MMP technology applied in modern nanotechnology. As a practical example, we designed and constructed an intelligent multilevel hierarchy with bacteria/cell recognition and irradiation attenuation capabilities. Though still preliminary, MMP exhibited impressive accuracy, consistency, universality, and three-dimensional tunability. It is an ideal process without expensive catalysts, extreme conditions, or extra pollutions. Most importantly, the unique reproducible property of MMP could significantly improve both the quality and production yield of APM, which in turn, would bring more high performance and low cost products to the marketplace, making our daily life more productive, convenient, and healthy.

EXPERIMENTAL SECTION

Characterization. Scanning electron microscopy (SEM) coupled with an energy dispersive spectroscopy (EDS) analysis were taken using Philips XL 30 and a JEOL JSM-6700F microscope. The microbiological toxicity of the samples was studied by a Leica DMIRE 2 inverted microscope. X-ray diffraction (XRD) patterns of the prepared samples were recorded on a Rigaku-Dmax 2500 diffractometer equipped at a scanning speed of 4°/min in the range from 30° to 65°. Transmission electron microscopy (TEM) and selected area electron diffraction (SAED) measurement was carried out with JEM-2000 FX. Optic images were obtained using Panasonic DMC-ZS1 camera. Electromagnetic radiation was studied by LZT-1160 EMF tester.

The Operation of MMP. In a typical experiment, the substrate was ultrasonicated consecutively in acetone, ethanol, and deionized water each for 20 min. After being dried in the microwave region (500 W, 20 s × 3 times), it was covered by layers of proper-sized filter (polypropylene filter, 80 mm in diameter, 2 mm in thickness, 2−15 μm in pore size, purchased from Qinyuan Company). Then the mixture of water, ethanol, and magnetic nanoparticles (Affimag PSC Magnetic Microspheres, 1, 2, 5, and 10 μm in diameter, purchased from BaseLine Company) was doped on the filter-covered substrate. They were fixed by the magnetic force and immersed into the solution with zinc nitrate hydrate (0.025 M) and HMTA (hexamethylenetetramine) (0.025 M)) at 80 °C for 12 h. The entire growth and patterning process was thus accomplished simultaneously. After that, magnetic nanoparticles were readily removed by switching the magnetic orientation. Subsequently, the obtained patterned membrane was removed from solution, immersed in deionized water (5 °C) immediately, and dried at 40 °C overnight.

MMP Printing Using Inkjet Printer. Canon PIXMA Pro9500 Mark II printer was used for printing of the microporous surface on PVC film. Three cartridges were filled with different sized magnetic

nanoparticles separately. After being preheated to 80 °C for the ease of processing, PVC films were covered with filters to disperse the inks. Those inks were then printed on the desired locations of the surface in a one-step operation.

ZnO Nest Loaded with Ag Decorated Magnetic Egg. Examethylenetetramine/ethanol (50 mM) solution was doped on the bandaid surface with $AgNO_3$ (0.05 g/L)-covered magnetic Fe_3O_4 nanoparticles (average diameter = 1.1 μm). After 12 h UV irradiation, the obtained taupe layer was fixed by using hot melt adhesive. Larger magnetic Fe_3O_4 nanoparticles (average diameter = 3 μm) were then dispersed on the taupe layer to form an upper ZnO nest by using MMP.

Cells Culture. Bacteria are potentially hazardous and should be treated carefully. Standard biosafe lab techniques were followed while handing them and the corresponding media. All microbiological toxicity tests were performed in triplicate to ensure reproducibility. Before the assays, bacterial cultures (*E.coli* and *S. aureus*) were grown in solid Luria−Bertani (LB) media overnight at 37 °C with continuous shaking at 200 rpm. The HEK293 cells were maintained in DMEM medium supplemented with 10% fetal calf serum (FCS), 1 mM sodium pyruvate, 2 mM glutamine, 50 U/mL penicillin, 50 mg/mL streptomycin, and 100 mM nonessential amino acids. The medium was exchanged once per 2 days. Before the assays, the cells were incubated in a humidified incubator at 37 °C and 5% CO_2 atmosphere for 2 days.

Microbiological Toxicity Tests. APM coated on substrate (1 cm × 1 cm) was used directly as additives for toxicity test. The HEK 293 cells were first washed three times by using DMEM without serum to get rid of the unattached cells, then 2 mL of cells solution were added into each well the 24-well plates, and the images were taken at certain areas from the wells in order to count the number of cells before incubation, followed by locating different membranes of nanostructures on the bottom of the wells. All the samples were incubated at 37 °C in 5% CO_2 incubator. After certain hours of incubation, the cells were washed five times by using Dulbecco's phosphate buffered saline (DPBS). Then 1 mL of DMEM was added into the wells as nutrition medium. The images of cells after incubation were taken from the same area as that before incubation. To evaluate the cytotoxicity of the nanostructures, fluorescent probes (Syto 9/PI) were used to access the live and dead cells. All the samples were studied by a Leica DMIRE 2 inverted microscope. For bacterial cultures, equal densities of *S. aureus* and *E. coli* (based on OD600 nm values) were used to inoculate LB broth with different substrates. Broth cultures were incubated with shaking, and viable cell densities were measured *via* FITC/PI staining. Green fluorescence was detected at 488 nm excitation with a band-pass filter ranging between 505 and 530 nm. Simultaneously, red fluorescence was detected using the long pass filter at 585 nm, and superimposition of both green and red fluorescence generated the final images. After treatment with different substrates for the same time, the cells in different wells were counted, respectively, and then 5×10^5 cells were transferred to the polypropylene centrifuge tubes for mitochondrial activity assessment. The activity was measured by using the 3-(4,5-dimethyl-thiazoyl-2)-2, 5-diphenyl tetrazolium bromide (MTT) method (Bouillaguet *et al*., 2000). Each experiment was done in triplicate. The average mitochondrial (SDH) activity per cell was expressed as a percentage of the control cultures.

Acknowledgment. This work was supported by the National Natural Science Foundation of China (No.20890022), the National Key Basic Research Development Project of China (No. 2010CB933602), and (No. 2007CB714500).

Supporting Information Available: Details of the materials and method. This material is available free of charge *via* the Internet at http://pubs.acs.org.

REFERENCES AND NOTES

1. Zhao, Y.; Wei, Min.; Lu, Jun.; Wang, L.; Duan, Xue. Biotemplated Hierarchical Nanostructure of Layered Double Hydroxides with Improved Photocatalysis Performance. *ACS Nano* **2009,** *3*, 40090–4016.
2. Huang, J.; Wang, X.; Wang, X.; Wang, Z. L. Controlled Replication of Butterfly Wings for Achieving Tunable Photonic Properties. *Nano Lett.* **2006,** *6*, 2325–2331.
3. Lei, J.; Zhao, Y.; Zhai, J. A Lotus-Leaf-like Superhydrophobic Surface: A Porous Microsphere/Nanofiber Composite Film Prepared by Electrohydrodynamics. *Angew. Chem., Int. Ed.* **2004,** *43*, 4338–4341.
4. Potyrailo, R. A.; Ghiradella, H.; Vertiatchikh, A.; Dovidenko, K.; Cournoyer, J. R.; Olson, E. Morpho Butterfly Wing Scales Demonstrate Highly Selective Vapour Response. *Nat. Photonics* **2007,** *1*, 123–128.
5. Weatherspoon, M. R.; Cai, Y.; Crne, M.; Srinivasarao, M.; Sandhage, K. H. 3D Rutile Titania-Based Structures with Morpho Butterfly Wing Scale Morphologies. *Angew. Chem., Int. Ed.* **2008,** *47*, 7921–7923.
6. Sethi, S.; Ge, L.; Ci, L.; Ajayan, P. M.; Dhinojwala, A. Gecko-Inspired Carbon Nanotube-Based Self-Cleaning Adhesives. *Nano Lett.* **2008,** *8*, 822–825.
7. Geim, A. K.; Dubonos, S. V.; Grigorieva1, I. V.; Novoselov, K. S.; Zhukov, A. A.; Shapoval, S. Yu. Microfabricated Adhesive Mimicking Gecko Foot-Hair. *Nat. Mater.* **2003,** *2*, 461–463.
8. Naik, R. R.; Stone, M. O. Integrating Biomimetics. *Mater. Today* **2005,** *8*, 18–26.
9. Sidorenko, A.; Krupenkin, T.; Taylor, A.; Fratzl, P.; Aizenberg, J. Reversible Switching of Hydrogel-Actuated Nanostructures into Complex Micropatterns. *Science* **2007,** *315*, 487–490.
10. Zhang, H.; Hussain, I.; Brust, M.; Butler, M. F.; Rannard, S. P.; Cooper, A. I. Aligned Two- and Three-Dimensional Structures by Directional Freezing of Polymers and Nanoparticles. *Nat. Mater.* **2005,** *4*, 787–793.
11. Xu, S.; Wei, Y.; Kirkham, M.; Liu, J.; Mai, W.; Davidovic, D.; Snyder, R. L.; Wang, Z. L. Patterned Growth of Vertically Aligned ZnO Nanowire Arrays on Inorganic Substrates at Low Temperature without Catalyst. *J. Am. Chem. Soc.* **2008,** *130*, 14958–14959.
12. Cheng, W.; Park, N.; Walter, M. T.; Hartman, M. R.; Luo, D. Nanopatterning Self-Assembled Nanoparticle Superlattices by Moulding Microdroplets. *Nat. Nanotechnol.* **2008,** *3*, 682–690.
13. Santhanam, V.; Andres, R. P. Microcontact Printing of Uniform Nanoparticle Arrays. *Nano Lett.* **2004,** *4*, 41–44.
14. Wang, X.; Zhu, H.; Yang, F.; Yang, X. Biofilm-Engineered Nanostructures. *Adv. Mater.* **2009,** *21*, 2815–2818.
15. Lu, A. H.; Salabas, E. L.; Schüth, F. Magnetic Nanoparticles: Synthesis, Protection, Functionalization and Application. *Angew. Chem., Int. Ed.* **2007,** *46*, 1222–1244.
16. Lin, C.; Li, Y.; Yu, M.; Yang, P.; Lin, J. A Facile Synthesis and Characterization of Monodisperse Spherical Pigment Particles with a Core/Shell Structure. *Adv. Funct. Mater.* **2007,** *17*, 1459–1465.
17. Feng, J.; Song, S.; Deng, R. P.; Fan, W. Q.; Zhang, H. Novel Multifunctional Nanocomposites: Magnetic Mesoporous Silica Nanospheres Covalently Bonded with Near-Infrared Luminescent Lanthanide Complexes. *Langmuir* **2010,** *26*, 3596–3600.
18. Isojima, T.; Lattuada, M.; Vander, Sande, J. B.; Hatton, T. A. Reversible Clustering of Ph- and Temperature-Responsive Janus Magnetic Nanoparticles. *ACS Nano* **2008,** *2*, 1799–806.
19. Liong, M.; Lu, J.; Kovochich, M.; Xia, T.; Ruehm, S. G.; Nel, A. E.; Tamanoi, F.; Zink, J. I. Multifunctional Inorganic Nanoparticles for Imaging, Targeting, and Drug Delivery. *ACS Nano* **2008,** *2*, 889–896.
20. Greene, L. E.; Yuhas, B. D.; Law, M.; Zitoun, D.; Yang, P. Solution-Grown Zinc Oxide Nanowires. *Inorg. Chem.* **2006,** *45*, 7535–7543.
21. Wang, Z. L. Splendid One-Dimensional Nanostructures of Zinc Oxide: A New Nanomaterial Family for Nanotechnology. *ACS Nano* **2008,** *2*, 1987–1992.
22. Xia, T.; Kovochich, M.; Liong, M.; Mädler, L.; Gilbert, B.; Shi, H.; Yeh, J. I.; Zink, J. I.; Nel, A. E. Comparison of the Mechanism of Toxicity of Zinc Oxide and Cerium Oxide Nanoparticles Based on Dissolution and Oxidative Stress Properties. *ACS Nano* **2008,** *2*, 2121–2134.

23. Dwivedi, P. D.; Misra, A.; Shanker, R.; Das, M. Are Nanomaterials a Threat to The Immune System?. *Nanotoxicology* **2009,** *3*, 19–26.
24. Feychting, M.; Ahlbom, A.; Kheifets, L. EMF and Health. *Annu. Rev. Public Health* **2005,** *26*, 165–189.
25. Becheri, A.; Dürr, M.; Nostro, P. L.; Baglioni, P. Synthesis and Characterization of Zinc Oxide Nanoparticles: Application to Textiles as UV-Absorbers. *Inorg. Chem.* **2005,** *44*, 3926–3930.